An activating deletion variant in the submembrane region of natriuretic peptide receptor-B causes tall stature

Lauffer, P.; Miranda-Laferte, E.; Duyvenvoorde, H.A. van; Haeringen, A. van; Werner, F.; Boudin, E.; ... ; Kaay, D.C.M. van der

An Activating Deletion Variant in the Submembrane Region of Natriuretic Peptide Receptor-B Causes Tall Stature

Peter Lauffer,[1,2,*] Erick Miranda-Laferte,[3,*] Hermine A. van Duyvenvoorde,[1] Arie van Haeringen,[1] Franziska Werner,[3] Eveline Boudin,[4] Hannes Schmidt,[5] Thomas D. Mueller,[6] Michaela Kuhn, [3,*] and Daniëlle C. M. van der Kaay[7,*]

[1]Department of Clinical Genetics, Leiden University Medical Center, 2333 ZA Leiden, the Netherlands; [2]Department of Paediatric Endocrinology, Emma Children's Hospital, Amsterdam University Medical Center, 1105 AZ Amsterdam, the Netherlands; [3]Institute of Physiology, University of Würzburg, 97070 Würzburg, Germany; [4]Centre of Medical Genetics, University of Antwerp, 2650 Edegem, Belgium; [5]Interfaculty Institute of Biochemistry, University of Tübingen, Tübingen 72076, Germany; [6]Department of Molecular Plant Physiology and Biophysics, Julius-von-Sachs-Institute, Biocenter, University of Würzburg, Würzburg 97070, Germany; and [7]Department of Paediatrics, Haga Hospital/Juliana Children's Hospital, 2545 AA The Hague, the Netherlands

ORCiD numbers: 0000-0002-1174-7340 (P. Lauffer); 0000-0003-4818-6804 (E. Boudin).

Context: C-type natriuretic peptide (CNP) is critically involved in endochondral bone growth. Variants in the genes encoding CNP or its cyclic guanosine monophosphate (cGMP)-forming receptor (natriuretic peptide receptor-B [NPR-B], gene *NPR2*) cause monogenic growth disorders. Here we describe a novel gain-of-function variant of NPR-B associated with tall stature and macrodactyly of the great toes (epiphyseal chondrodysplasia, Miura type).

Design: History and clinical characteristics of 3 family members were collected. *NPR2* was selected for sequencing. Skin fibroblasts and transfected HEK-293 cells were used to compare mutant versus wild-type NPR-B activities. Homology modeling was applied to understand the molecular consequences of the variant.

Results: Mother's height was +2.77 standard deviation scores (SDS). The heights of her 2 daughters were +1.96 SDS at 7 years and +1.30 SDS at 4 years of age. Skeletal surveys showed macrodactyly of the great toes and pseudo-epiphyses of the mid- and proximal phalanges. Sequencing identified a novel heterozygous variant c.1444_1449delATGCTG in exon 8 of *NPR2*, predicted to result in deletion of 2 amino acids Met482-Leu483 within the submembrane region of NPR-B. In proband's skin fibroblasts, basal cGMP levels and CNP-stimulated cGMP production were markedly increased compared with controls. Consistently, assays with transfected HEK-293 cells showed markedly augmented baseline and ligand-dependent activity of mutant NPR-B.

Conclusions: We report the second activating variant within the intracellular submembrane region of NPR-B resulting in tall stature and macrodactyly. Our functional and modeling studies suggest that this domain plays a critical role in the baseline conformation and ligand-dependent structural rearrangement of NPR-B required for cGMP production. **(*J Clin Endocrinol Metab* 105: 2354–2366, 2020)**

Key Words: natriuretic peptide receptor-B, guanylyl cyclase B, C-type natriuretic peptide, cyclic GMP, tall stature, macrodactyly

ISSN Print 0021-972X ISSN Online 1945-7197
Printed in USA

Received 18 December 2019. Accepted 10 April 2020.
First Published Online 16 April 2020.
Corrected and Typeset 28 May 2020.

*P.L. and E.M.-L. contributed equally; M.K. and D.C.M.vd.K. contributed equally.
Abbreviations: 3D, 3-dimensional; cGMP, cyclic guanosine monophosphate; CNP, C-type natriuretic peptide; ECD, extracellular domain; IBMX, 3-isobutyl-1-methylxanthine; NP, natriuretic peptide; NPR, natriuretic peptide receptor; PDE, phosphodiesterase; SDS, standard deviation score; WT, wild-type.

C-type natriuretic peptide (CNP), the third discovered member of the natriuretic peptide (NP) family, received its name because it shares a common amino acid core structure with the previously isolated cardiac hormones atrial and B-type NPs (ANP and BNP) (reviewed in (1)). However, human and murine genetic studies later revealed that CNP's major physiological function is not the regulation of renal natriuresis. Instead, CNP is a critical regulatory hormone in the bone, where it stimulates physiological endochondral bone growth by auto/paracrine activation of its specific cyclic GMP-forming natriuretic peptide receptor-B (NPR-B, also named guanylyl cyclase-B) in chondrocytes (1-3). In addition, local CNP/NPR-B signalling participates in oocyte maturation, sensory axon bifurcation, and moderation of arterial blood pressure (1, 4, 5).

NPR-B presents as a homodimer, and each subunit contains an extracellular CNP-binding domain, a short transmembrane region and an intracellular region with a short submembrane segment followed by a kinase homology regulatory domain, a coiled-coil dimerization region and a C-terminal guanylyl cyclase domain (1, 6). After extracellular binding of CNP, the intracellular guanylyl cyclase domain catalyses the conversion of guanosine triphosphate to cyclic guanosine monophosphate (cGMP) as a second messenger. In chondrocytes, this fosters hypertrophy, differentiation, and extracellular matrix deposition necessary for longitudinal bone growth (2, 3). The kinase-like domain does not exert kinase activity; however, phosphorylation of specific residues within this region is necessary for CNP-dependent stimulation of cGMP synthesis (6).

The essential role of the chondrocyte CNP/NPR-B/cGMP signalling pathway during long bone growth has been demonstrated in many functional and genetic studies. In mice, global or chondrocyte-restricted CNP (gene name *Nppc*) or NPR-B (*Npr2*) deletions provoke severe dwarfism (3, 7). In human, homozygous or compound heterozygous loss-of-function variants of NPR-B (MIM #108961) lead to extreme short stature, with shortening of the limbs, severe brachydactyly of the hands and feet, and skeletal dysplasia, a condition named acromesomelic dysplasia, type Maroteaux (AMDM, MIM #602875) (8). Consistently, heterozygous loss-of-function NPR-B variants are associated with mildly reduced stature (MIM #616255) (9, 10). Conversely, gain-of-function NPR-B variants lead to tall stature, sometimes associated with a Marfanoid habitus, arachnodactyly, and scoliosis, a condition named epiphyseal chondrodysplasia, Miura type (MIM #615923) (11-13). Three such intracellular activating variants of NPR-B have been identified in humans: the Val883Met variant is located in the cyclase domain (11); the Ala488Pro and Arg655Cys variants affect the submembrane and kinase-homology domains, respectively (12, 13). Because such variants enhanced both the basal and CNP-stimulated cGMP-synthesis of NPR-B, it was suggested that they provoke a conformational change which is similar to that adopted by NPR-B in response to CNP binding (14).

In this report, we describe a novel heterozygous gain-of-function variant c.1444_1449delATGCTG in exon 8 of *NPR2*, predicted to result in the deletion of 2 amino acids Met482-Leu483 in the cytosolic submembrane region of NPR-B. Similarly to the previously identified Ala488Pro variant in this region (12), this novel variant is associated with tall stature and macrodactyly of the great toes (epiphyseal chondrodysplasia, Miura type).

Research Design and Methods

Patients

We studied a family of Dutch origin, including a mother and her 2 daughters. Informed consent and assent were obtained from the 3 probands. Blood samples were obtained from the mother and saliva was obtained from her daughters for genotyping. Fibroblasts from a skin biopsy were obtained from the mother for ex vivo studies of NPR-B activity. We compared fibroblast NPR-B expression and activity with fibroblasts from a wild-type (WT) NPR-B healthy volunteer and with the previously described proband with the activating Arg655Cys NPR-B variant (13).

Sanger sequencing and analysis

DNA was isolated from blood samples using the chemagic Prime instrument (PerkinElmer, Waltham, MA, USA). DNA from saliva was isolated using the prepIT-L2P kit (DNA Genotek, Kanata, Ontario, Canada). Primer design for *NPR2* was based on a template sequence available on Ensembl transcript ENST00000342694.6 and ENST00000265074.13, respectively. Primers were designed for all coding exons and the corresponding intron/exon boundaries using Primer3, version 4.1.0 (sequences available upon request). Amplification of the selected gene regions was performed using GoTaq G2 DNA polymerase-mediated PCR (Promega Corporation, Madison, WI, USA) and was verified by agarose gel electrophoresis. Primer sequences and PCR conditions are available on request. After amplification by PCR, primers, and unincorporated dNTPs (Promega Corporation) were removed using exonuclease I (New England Biolabs, Inc, Ipswich, MA, USA) and calf intestine alkaline phosphatase (CIAP,

Roche Applied Science, Hoffmann–La Roche AG, Basel, Switzerland). Sequencing was carried out directly on purified fragments with the ABI 310 Genetic Analyzer (Applied Biosystems, Foster City, CA, USA), using an ABI Prism BigDye terminator cycle sequencing ready reaction kit, version 1.1 (Applied Biosystems). The BigDye XTerminator purification kit was used as purification method for DNA sequencing with the purpose of removing unincorporated BigDye terminators. The presence of the *NPR2* variant in both affected daughters was also confirmed using Sanger sequencing.

Isolation and culture of skin fibroblasts and cGMP determinations

Skin biopsies were taken from the proband and a healthy 37-year-old female (height 171 cm, +0.07 standard deviation score [SDS]), and fibroblast cultures were established as previously described (13). Fibroblasts of the previously described proband (not related to the currently investigated family) with the activating Arg655Cys NPR-B variant were included for comparison (13). Experiments were performed in mitogen-free, serum-reduced DMEM (0.5% fetal calf serum 4 hours before experimentation). Cells were pretreated with 0.1 mM of the phosphodiesterase inhibitor 3-isobutyl-1-methylxanthine (IBMX; Sigma) for 15 minutes, and then stimulated with CNP (0.1-100 nM; Bachem) for another 10 minutes. Intracellular cGMP contents were extracted with 70% (v/v) ice-cold ethanol and determined by radioimmunoassay (5, 13).

Site-directed mutagenesis and cGMP responses of transfected HEK-293 cells to CNP

To generate the construct encoding the mutant protein NPR-B Met482-Leu483del, a PCR fragment was amplified from a *pFLAG-CMV1* vector containing the WT *NPR2* cDNA (Swiss-Prot entry Q6VVW5 (13)). The reverse primer: 5- CCATAG CATGCTAGCCAGCTCCTTCTCCAGCTTCCG GAAAATTAGGAAACTG-3, spanning the novel c.1444_1449delATGCTG deletion, and the forward primer: 5-GGGCACTTCAATTGGACAGCTCG-3 were used for the PCR amplification. The PCR fragment containing the variant was digested with the MfeI and NheI restriction enzymes, and subcloned into the *pFLAG-CMV1-NPR2* vector restricted with the same enzymes. The desired variant and the absence of unwanted variants were verified by sequencing.

To compare the expression and activity levels of the WT and mutant NPR-B proteins, HEK-293 cells were transiently transfected with 10 µg of the respective plasmids in 10-cm dishes using the *X-tremeGene HP* DNA transfection reagent (Roche). For immunoblotting, membrane proteins were isolated 48 hours posttransfection. To assess intracellular cGMP responses, the HEK-293 cells were transferred into 24-well plates (100 000 cells per well) 1 day after transfection (13). After 20 hours, the cells were serum starved for 4 hours, pretreated with 0.1 mM IBMX for 15 minutes, and then incubated with various concentrations of CNP for another 10 minutes. Intracellular cGMP contents were determined as stated previously (5, 13).

Guanylyl cyclase activity assays

Guanylyl cyclase activity of crude membranes prepared from transfected HEK-293 cells was assessed as described before (13). Assays were performed in a 50 mM HEPES buffer, pH 7.4, containing 50 mM NaCl, 5% glycerol, 0.05% BSA, 1 mM IBMX, 2 mM guanosine triphosphate, 30 mM creatine phosphate, 1.5 U/mL creatine phosphokinase, and 2 mM ATP. Membranes (20 µg protein) were incubated with CNP (to assess ligand-dependent activity), or with 1% (v/v) Triton X-100 (for detergent stimulated, maximal activity) during 10 minutes (13). cGMP formation was measured by radioimmunoassay (5, 13). Basal and CNP-stimulated cGMP responses were calculated as percentage of maximal Triton-stimulated activity.

Cell membrane fractionations and western blotting

Membrane protein fractions were obtained from cultured skin fibroblasts and HEK-293 cells using a Protein Fractionation Kit (Thermo Fisher Scientific). For Western blot analyses, 25 µg protein was resolved by sodium dodecyl sulfate-PAGE (13). The primary antibodies were against NPR-B (1:5000 (5);) and Na^+/K^+-ATPase (1:5000; Abcam).

In silico modelling

To elucidate the possible impact of the reported Met482-Leu483 deletion within the intracellular membrane near region of NPR-B (UniProt code P20594) a theoretical 3-dimensional (3D) model was built for the region spanning Thr451 to Arg495. First, the location of the transmembrane helix of NPR-B was predicted using the software tool TMHMM 2. 0 (http://www.cbs.dtu.dk/). Subsequently, secondary structure prediction was performed for the region comprising residues Leu456 to Trp492 using the software JPRED4 (http://www.compbio.dundee.ac.uk). A 3D model was then built using the software package Quanta2008 (BIOVIA, San Diego, CA, USA) and the tool ProteinDesign. A 3D model for the

deletion variant was similarly obtained by the building routine using Quanta2008/ProteinDesign removing residues Met482 and Leu483.

Statistical analyses

Data are presented as mean ± SEM. The 2-tailed unpaired Student *t*-test was used to analyze significant differences between 2 groups. $P < 0.01$ was considered significant.

Results

Clinical characteristics and investigations

The proband is a currently 37-year-old female. She was born at term to nonconsanguineous parents after a normal pregnancy with a birth weight of 3400 g (-0.39 SDS) and a birth length of 49 cm (-0.92 SDS). She reached developmental milestones at appropriate ages. At the age of 8 years, she was treated for the first time for markedly long great toes by bilateral percutaneous epiphysiodesis. Throughout adolescence, the proband exhibited tall stature and low weight for height. At 14 years of age, her height was 181 cm, bone age was 13 years according to Greulich and Pyle, and predicted adult height was 186.8 cm based on the Bayley-Pinneau tables. Physical examination at that time showed macrodactyly of the great toes, long thumbs, an arm span to height ratio of 0.9, and a positive "thumb sign" (a sign of arachnodactyly; positive if the distal phalanx of the thumb reaches beyond the ulnar border of the palm, after wrapping the fingers around the thumb in adduction) without other signs of Marfan syndrome. Family history was unremarkable except for osteoporosis in the proband's mother and grandmother. The proband's parents and brother are of normal height. From age 14 years, she was treated with supraphysiological doses of estrogens (200 mcg of ethinylestradiol per day) in combination with progesterone (5 mg of hydroxyprogesterone during the first 10 days of each month) for adult height reduction. Menarche occurred 3 months after start of treatment. Treatment had little effect on her growth and was discontinued at the age of 16 years. The proband has been experiencing irregular menses since menarche (menses every 25-60 days). She has had 2 spontaneous pregnancies and possibly 1 miscarriage.

Table 1. Anthropometric Data

	H (HSDS)	SHHR (SDS)	AHR
Proband	188.1 cm (+2.8)	0.50 (-1.7)	0.90
Daughter 1	136.8 cm (+2.0)	0.53 (-0.5)	0.94
Daughter 2	110.2 cm (+1.3)	0.54 (-0.7)	0.94

Daughter 1: eldest daughter (age 7.1 years), daughter 2: youngest daughter (age 4.0 years). Abbreviations: AHR, arm span to height ratio; H, height; SDS, standard deviation scores; SHHR, sitting height to height ratio.

The proband is presently diagnosed with fibromyalgia and monitored by a rheumatologist. Her current anthropometric data are shown in Table 1. She has a minor ankle valgus, no scoliosis, and no joint hypermobility. She reports nearsightedness, with a correction of -5 diopters. Arterial blood pressure is normal.

The proband and her nonconsanguineous spouse gave birth to 2 daughters. The girls were born at term following uneventful pregnancies. Birth weight of the eldest daughter at 38 + 1 weeks gestation was 2740 g (-1.13 SDS); length at 1 month was 53.5 cm (-0.13 SDS). She reached developmental milestones at an appropriate age, except for idiopathic toe walking until the age of 3 years. She has pes planovalgus. She underwent epiphysiodesis of both great toes when she was 5 years old. She wears glasses (+3.75/+3.5). The youngest daughter was born at 37 + 2 weeks gestation with a birth weight of 2740 g (-0.66 SDS); length at the age of 5 weeks was 54 cm (-0.43 SDS). She has a history of minor gross motor developmental delay and receives speech therapy. They were referred for clinical genetic evaluation at the age of 6 and 4 years, respectively, because of progressive macrodactyly of the great toes. At physical examination, the girls had markedly long great toes (Fig. 1), ankle valgus, and long thumbs with a positive thumb sign. Skeletal surveys of the girls demonstrate pseudo-epiphyses of mid- and proximal phalanges in hands and feet, but not in other long bones (Fig. 1). Beighton score (joint hypermobility score in which a maximum of 9 points can be allocated for specific maneuvers; ≥ 4 points indicates generalized hypermobility) was 0 in both girls. No specific facial dysmorphic features were noted. At anthropometric evaluation, the girls had a diminished span to height ratio resulting from shortened forearms (mesomelia). For current anthropometric data, see Table 1 and Fig. 1. The father of the girls is 178 cm (-0.58 SDS), which results in a target height of 175 cm (+0.68 SDS) with a range of 165 to 185 cm. Skeletal surveys of the girls showed pseudo-epiphyses of the mid- and proximal phalanges of all fingers and both great toes (Fig. 1). The growth curve of the eldest daughter shows progressive growth acceleration until the age of 4.5 years up to a height of +2 SDS (Fig. 2A); the curve of the youngest daughter seems to follow this pattern (Fig. 2B). Bone age was

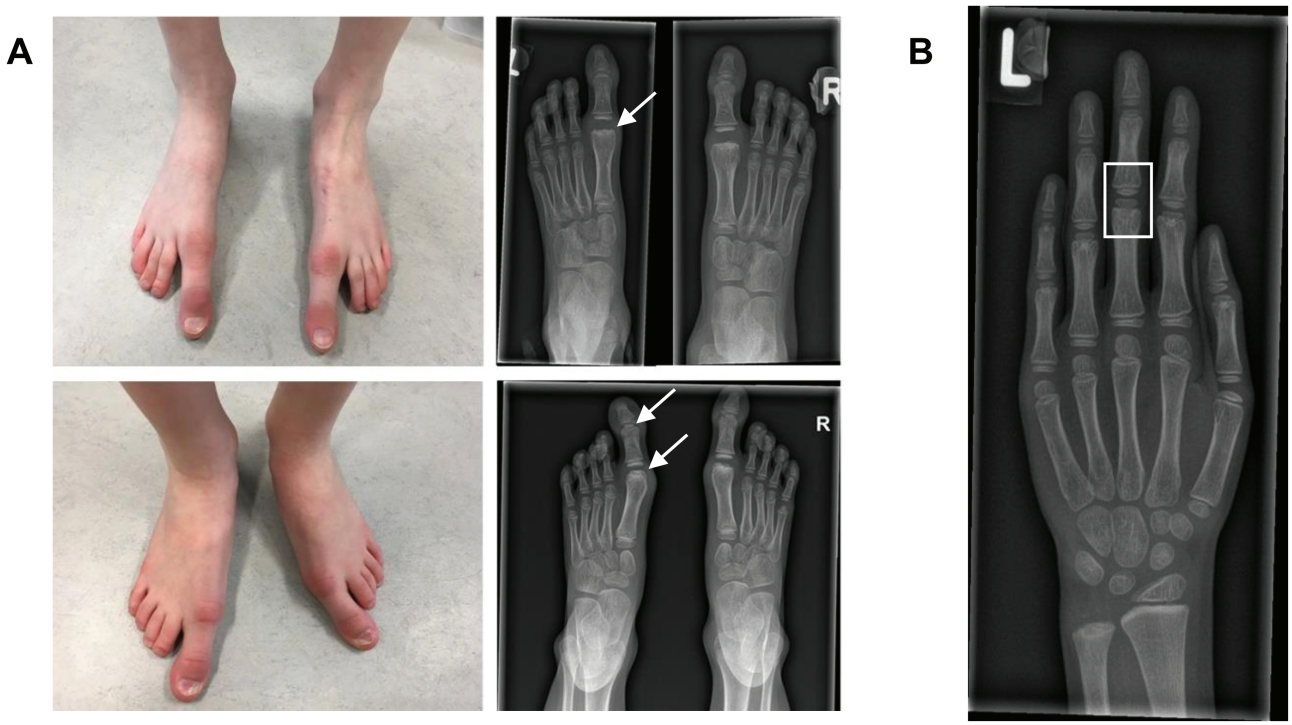

Figure 1. Photographs and radiographs of the feet and hand of the proband´s daughters. (A) Macrodactyly of the great toes of the eldest (upper panels) and youngest daughter (lower panels). The radiograph of the eldest daughter shows iatrogenic bone abnormalities on the distal part of metatarsal 1 after ablation of the pseudo-epiphyses (upper panel; white arrow). The pseudo-epiphyses in the first metatarsophalangeal joint and proximal interphalangeal joint of the youngest daughter are clearly distinguishable (lower panel; white arrows). (B) Left hand of the eldest daughter. The mid- and proximal phalanges of all fingers show pseudo-epiphyses (white square). Carpalia and metacarpals are normal.

according to calendar age in both girls. No other skeletal abnormalities were observed.

Identification of a heterozygous variant in the NPR2 gene

Because of the similarities with the phenotypes of the patients published by Miura et al. (11, 12), we selected *NPR2* as a candidate gene for further investigations. Sanger sequencing identified a heterozygous c.1444_1449delATGCTG deletion in exon 8 of *NPR2* (NM_003995.3), which is predicted to lead to an in-frame deletion of 2 highly conserved amino acids, methionine 482 and leucine 483, within the intracellular membrane near region of NPR-B (Fig. 3). The same heterozygous *NPR2* variant was sequenced in DNA of the daughters. Other family members were not studied. Fig. 3 illustrates that the amino acid sequence of this region of NPR-B is very conserved across species.

Fibroblasts from the proband with the Met482-Leu483del NPR-B variant have enhanced basal cGMP levels and augmented cGMP responses to CNP

To study the impact of the variant on the expression and activity of native NPR-B, we cultured fibroblasts from skin biopsies of the forearms of the proband and an age-/gender-matched control donor. Western blot analyses of fractionated membrane proteins revealed that membrane NPR-B expression levels were lower in the proband´s fibroblasts as compared to control (Fig. 4A). Despite this attenuated expression, the basal cGMP contents of such fibroblasts were significantly increased (Fig. 4B). Moreover, the cGMP responses to low, physiological CNP concentrations (0.1 and 1 nM) were significantly augmented (Fig. 4C). The effects of higher, supraphysiological CNP concentrations (10 and 100 nM) were also greater in fibroblasts from the proband; however, the difference to controls did not reach statistical significance (Fig. 4C). Although we could only study fibroblasts from 1 control donor, the results suggest increased baseline and ligand-evoked activity of the mutant NPR-B naturally expressed in fibroblasts.

Site-directed mutagenesis demonstrates enhanced baseline and CNP-stimulated guanylyl cyclase activity of the mutant NPR-B

Receptor-independent alterations may influence NPR-B activity in native cells. Therefore, we replicated the variant by site-directed mutagenesis for studies in a heterologous expression system. Transfection of HEK-293 cells with cDNA encoding Met482-Leu483del NPR-B produced slightly less amounts of

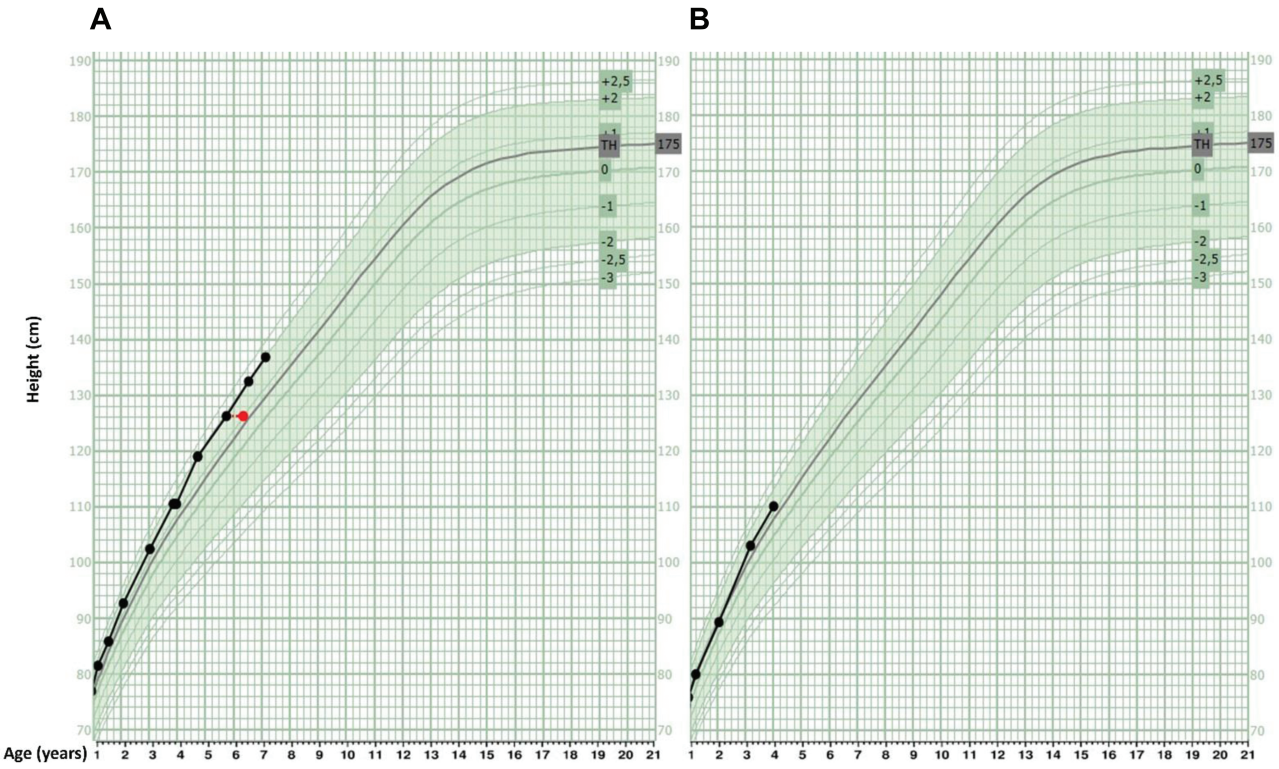

Figure 2. Growth curves of proband's daughters. The black lines represent growth data of the daughters. The green band represent population reference data (from -2 SDS to +2 SDS). Red dot: bone age at time of measurement. TH: target height. (A) The growth curve of the eldest daughter shows progressive growth acceleration until the age of 4.5 years up to a height of +2 SDS. (B) The curve of the youngest daughter also seems to follow this pattern.

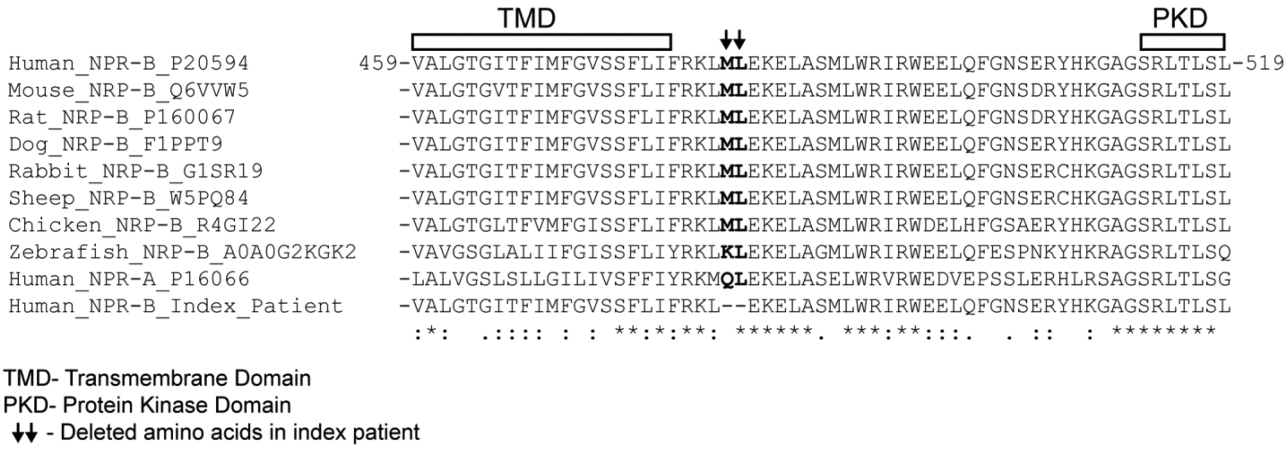

Figure 3. Alignments of the amino acids 459–519 of NPR-B comparing the sequences of wild-type NPR-B across species, human NPR1 and mutant NPR-B. TMD represents the transmembrane domain and PKD the start of the protein kinase-homology domain. The black arrows label the 2 amino acids (Met482-Leu483) that are deleted in the cytosolic sub-membrane region of NPR-B in the proband (last line). For comparison, the sequence of the human natriuretic peptide receptor type A (NPR-A, also named guanylyl cyclase-A [GC-A]) is also included. Please note the high sequence conservation of the trans- and submembrane regions of NPR-B among species and between NPR-B and NPR-A, which suggests that the here studied deletion variant affects a functionally critical region. NPR, natriuretic peptide receptor.

membrane-bound immunoreactive protein compared with WT NPR-B in 3 separate experiments (Fig. 5A). Together with the experiments with cultured fibroblasts this suggests diminished synthesis and/or membrane localization of the mutant. Despite, basal intracellular cGMP levels of HEK-293 cells expressing the mutant were ~9.9-fold higher in comparison with cells expressing WT NPR-B (Fig. 5B). CNP evoked concentration-dependent increases of intracellular cGMP levels. The responses to low CNP concentrations (0.01-1 nM CNP) were significantly greater in cells expressing the mutant, whereas the responses to a high CNP concentration (10 nM) were similar between cells expressing the WT or the mutant receptor (Fig. 5B).

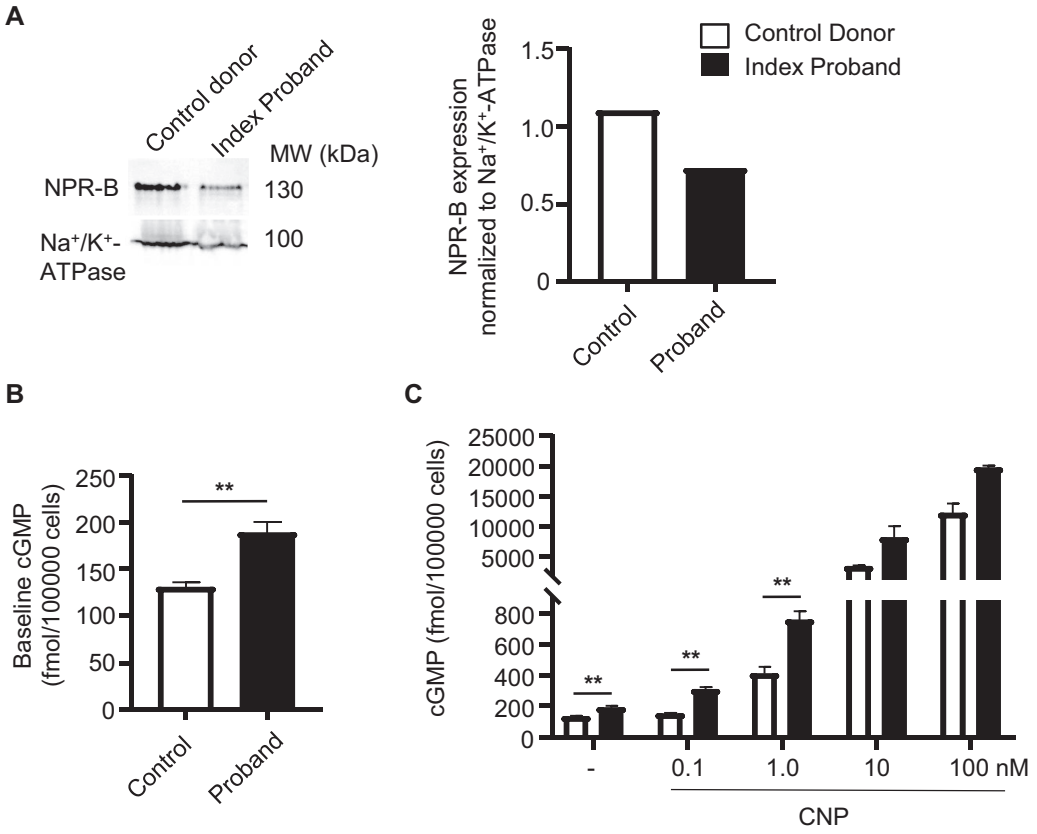

Figure 4. Cultured skin fibroblasts prepared from the proband have increased baseline cGMP levels and greater cGMP responses to CNP. (A) Western blot analysis of membrane NPR-B expression levels in fibroblasts cultured from a control donor and the proband. NPR-B expression was normalized to Na^+/K^+-ATPase expression. (B) Baseline intracellular cGMP levels of fibroblasts from the donor and the proband. (C) Effects of CNP on intracellular cGMP levels. Means ± SEM (n = 3); $^{**}P < 0.01$. cGMP, cyclic guanosine monophosphate; CNP, C-type natriuretic peptide; NPR, natriuretic peptide receptor.

Guanylyl cyclase activity assays were performed with crude membranes from transfected HEK-293 cells in the presence of 2 mM ATP to mimic cytoplasmic ATP levels. Such assays harbor the advantage that the response to CNP can be normalized to the maximal, detergent (Triton)-induced NPR-B activity. This facilitates the comparison of WT and mutant receptor activities when their membrane expression levels are unequal. Fig. 5C corroborates the previous experiments showing that baseline, ligand-independent activity of Met482-Leu483del NPR-B as well as the responses to low CNP concentrations (0.01-1 nM CNP) were significantly augmented. The responses to the highest CNP concentration (10 nM) were similar to the WT receptor (Fig. 5C). In concordance with the reduced protein expression levels, the maximal, Triton-stimulated activity of the mutant NPR-B was slightly reduced (Fig. 5C). To account for the differences in membrane receptor expression levels, within each experiment the CNP stimulated activity data were normalized to the respective maximal, Triton-stimulated NPR-B activity (considered as 100%) (Fig. 5D). This normalization demonstrated the mutant NPR-B exhibits augmented catalytic activity at baseline and in response to all tested CNP concentrations. In other words, the previous observations that the effects of high CNP concentrations (10-100 nM) on intracellular cGMP levels of fibroblasts (Fig. 4C) or HEK-293 cells (Fig. 5B) were similar between cells expressing WT or mutant NPR-B, is probably linked to the attenuated membrane expression of the mutant.

The Met482-Leu483del NPR-B variant has lower baseline and CNP-stimulated guanylyl cyclase activities than the Arg655Cys NPR-B variant

Last, we compared in fibroblasts and transfected HEK-293 cells the CNP responsiveness of the novel deletion variant with the previously published variant Arg655Cys (13). This point mutation variant, which we found in an extremely tall proband (13), affects the KHD of NPR-B. Fig. 6A illustrates that membrane NPR-B expression levels in fibroblasts cultured from both probands were lower, as in fibroblasts from the control donor. The cGMP-responses to a physiological CNP concentration (0.1 nM) were greatest in fibroblasts from the previously published proband with the Asp655Cys NPR-B variant (Fig. 6B).

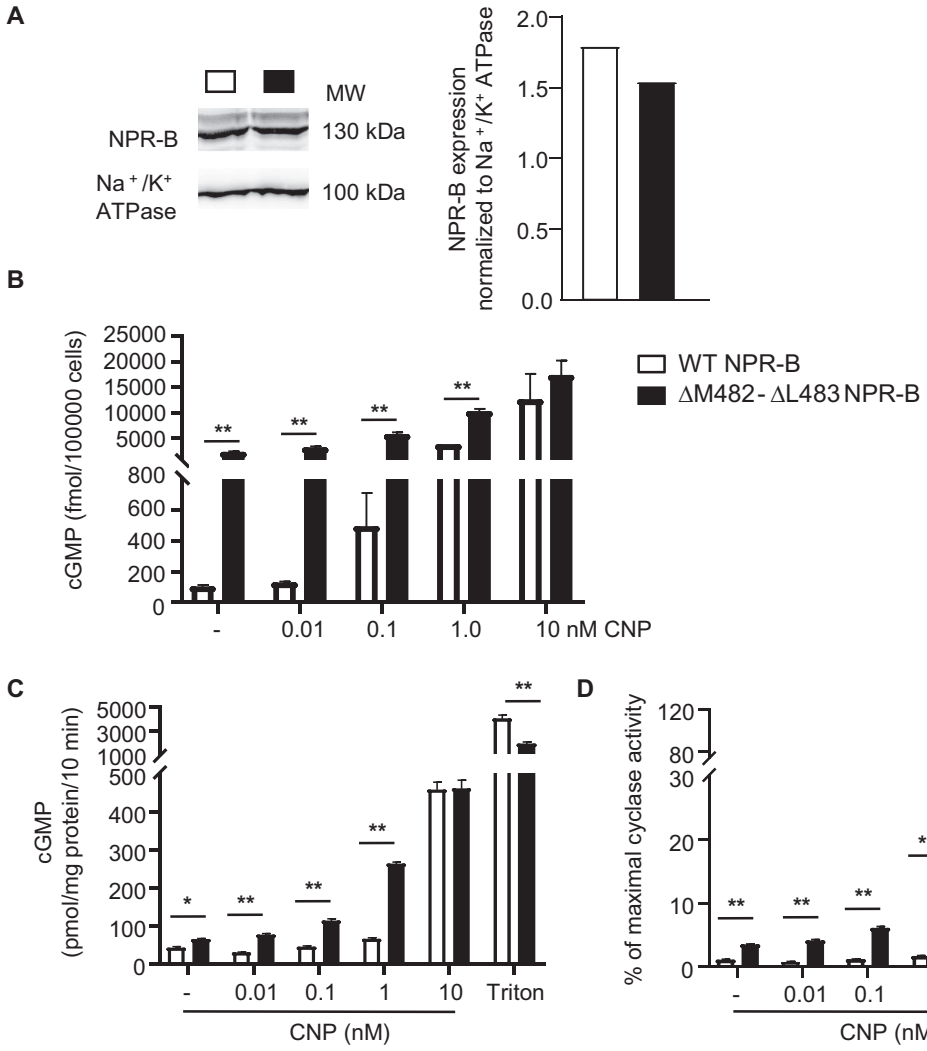

Figure 5. HEK-293 cells expressing the mutant Met482-Leu483del NPR-B exhibit increased baseline cGMP levels and greater cGMP responses to CNP. (A) Western blot analysis of membrane NPR-B expression levels in HEK-293 cells transfected with cDNA encoding WT or mutant NPR-B (10 µg DNA/dish). Expression was normalized to Na^+/K^+-ATPase expression. (B) Baseline intracellular cGMP levels (-) and effects of CNP on intracellular cGMP levels of HEK-293 cells expressing WT or mutant NPR-B. (C and D) Guanylyl cyclase activity assays with crude membranes prepared from cells expressing WT or mutant NPR-B. Membranes were incubated with vehicle (-), CNP or detergent (1% Triton X-100). cGMP production was measured by radioimmunoassay. In D, values are presented as percent of the maximal Triton-induced activity (as 100%). Means ± SEM (n = 3 independent experiments); $^{**}P < 0.01$. cGMP, cyclic guanosine monophosphate; CNP, C-type natriuretic peptide; NPR, natriuretic peptide receptor.

HEK-293 cells were transfected with the cDNAs encoding each mutant. Western blot analysis showed that the expression of the Met482-Leu483del NPR-B mutant was slightly lower than the expression of Arg655Cys NPR-B (Fig. 6C). Guanylyl cyclase activity assays using crude membranes from transfected HEK-293 cells revealed that Met482-Leu483del NPR-B has significantly lower baseline (ligand-independent) activity and lower responses to CNP compared with Arg655Cys NPR-B (Fig. 6D). As also shown, in concordance with the reduced protein expression levels, the maximal, Triton-stimulated activity of the Met482-Leu483del NPR-B mutant was also slightly lower. To account for such differences in membrane expression levels, the CNP-stimulated activity data were again normalized to the respective maximal, Triton-stimulated NPR-B activity. These evaluations confirmed that the Met482-Leu483del NPR-B mutant exhibits lower responsiveness to CNP as compared to the Arg655Cys NPR-B mutant (Fig. 6E).

Molecular modelling suggests that the Met482-Leu483 deletion changes the 3D structure of the submembrane region of NPR-B

Crystal structure analyses of the extracellular domain (ECD) of natriuretic peptide receptor-A (NPR-A), shared by ANP and BNP, provided insights into the molecular mechanisms of ligand recognition and a model of ligand-induced allosteric NPR-A activation (15, 16). These experimental studies revealed that ANP binding

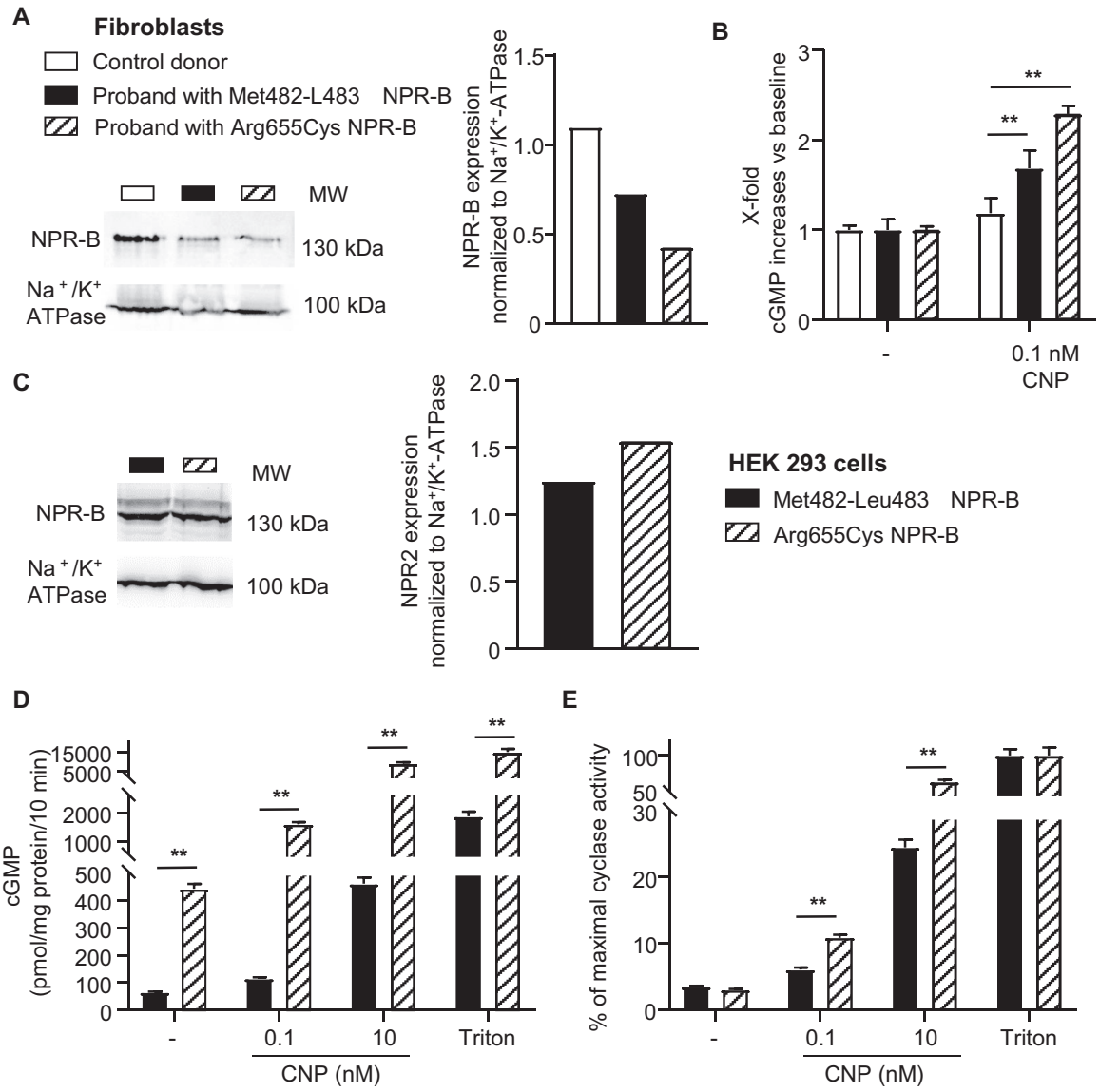

Figure 6. The mutant Met482-Leu483del NPR-B has lower basal and CNP-stimulated cGMP-synthesis activity compared with the previously published mutant Arg655Cys NPR-B. (A) Membrane NPR-B expression levels and (B) CNP (0.1 nM)-induced cGMP formation in fibroblasts cultured from a control donor or from the probands with either variant. (C) Western blot analysis of membrane NPR-B expression levels in HEK-293 cells expressing the Met482-Leu483del or Arg655Cys NPR-B mutants. NPR-B expression was normalized to Na^+/K^+-ATPase expression. (D and E) Guanylyl cyclase activity assays demonstrate that the mutant Met482-Leu483del NPR-B exhibits lower baseline enzymatic activity and lower cGMP responses to CNP compared with the mutant Arg655Cys. Crude membranes prepared from HEK-293 cells expressing either mutant were incubated with vehicle (-), CNP or detergent (1% Triton X-100). cGMP production was measured by radioimmunoassay. (E) Values are expressed as percent of the maximal Triton-induced activity (as 100%). Means ± SEM (n = 3); $^{**}P < 0.01$. cGMP, cyclic guanosine monophosphate; CNP, C-type natriuretic peptide; NPR, natriuretic peptide receptor.

induces a rotation of the ECDs of the 2 monomer subunits of the receptor dimer with respect to each other. It was postulated that this movement transduces across the membrane being an allosteric trigger for activation of the intracellular guanylyl cyclase domain to cGMP synthesis (15). Unfortunately, no experimentally validated structure is currently available for the transmembrane and intracellular regions of NPR-B or a homologous protein. To generate a working hypothesis about how the deletion of residues Met482-Leu483 could impact NPR-B activity, a theoretical 3D model of the transmembrane domain and the submembrane segment containing residues Met482-Leu483 was built using bioinformatic tools. Sequence-based tools to predict location and secondary structure indicated that the residues Leu456 to Phe478 form a single transmembrane helix, as expected for a type I transmembrane receptor (Fig. 3). This is consistent with the notion of basic positively charged amino acids at the C-terminal end of transmembrane helices (here, as residues Arg479 and Lys480), which are important to vertically fix such helices in the lipid bilayer (17). Subsequently secondary

structure modelling was performed for this transmembrane sequence and flanking extra- and intracellular protein segments. This predicted that the transmembrane and intracellular membrane near regions very likely form a continuous α-helical structure running from Leu456 to Trp492 (Fig. 7A). The 3D models were built to estimate how the deletion of residues Met482 and Leu483 would change these single helices. Because an α-helix has 3.6 residues per full turn, a 2-residue deletion would result in a reorientation of the helix surface ahead and past the deletion site by 120° (Fig. 7A, right panel; and Fig. 7B, left panel). The amphipathic signature of the helix markedly changes as a result of that. The 3D model of WT NPR-B indicated that this segment does not form a continuous hydrophobic patch, whereas in the Met482-Leu483 deletion variant, a continuous hydrophobic patch is predicted to run along the transmembrane region into the submembrane region (Fig. 7B, middle panel). Such change in the surface chemistry of this intracellular membrane-near segment of the here described mutant NPR-B might can affect dimer stability or conformation thereby leading to a

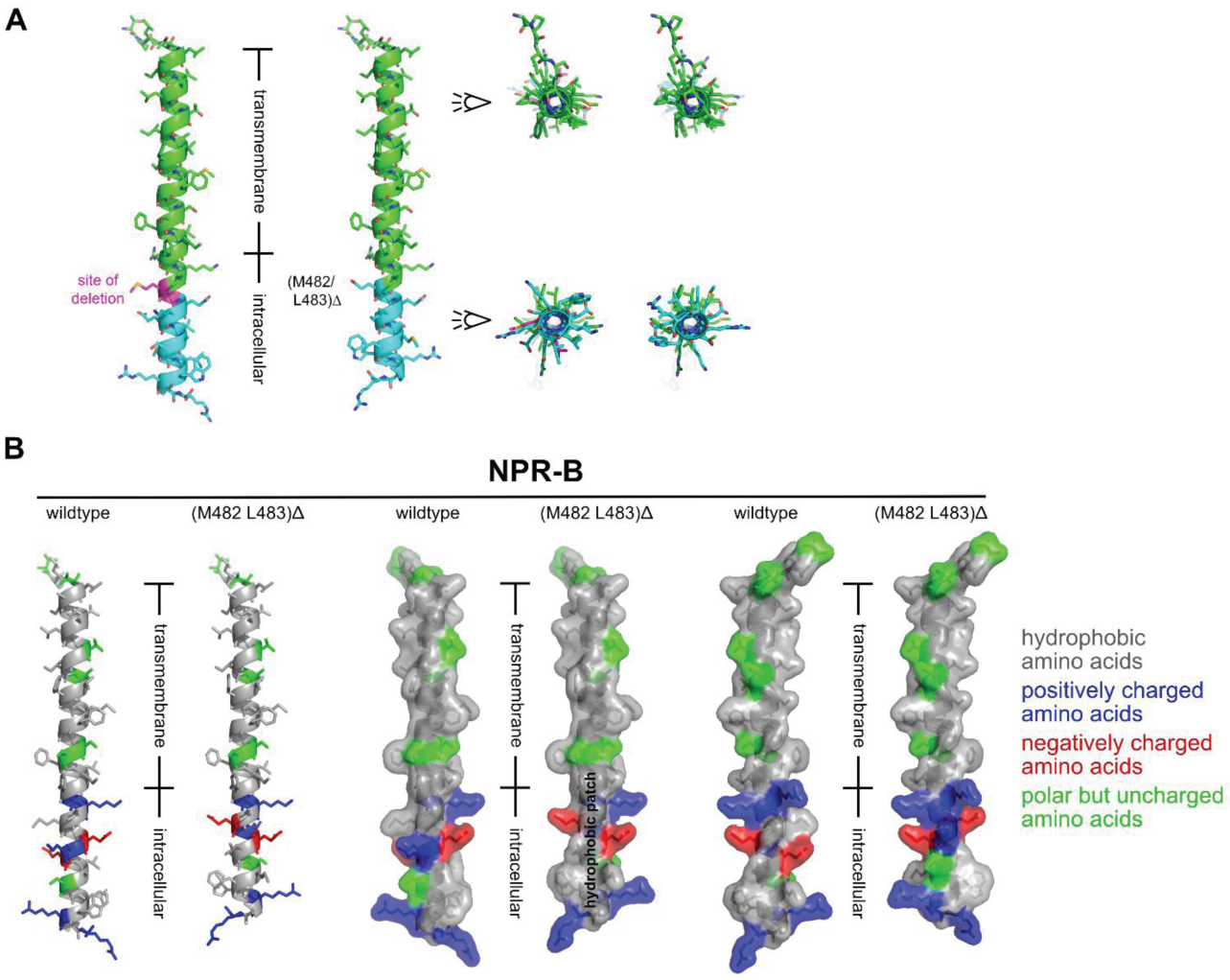

Figure 7. A theoretical 3D model of the trans- and cytosolic submembrane segments of WT and mutant NPR-B. Bioinformatic modelling predicted that Leu456 is the N-terminal start and Phe478 the end of the transmembrane region, which is consistent with the notion that basic residues at the C-term of transmembrane helices (here, residues Arg479 and Lys480) are important to vertically fix such helices in the lipid bilayer (17). Secondary structure prediction indicated an uninterrupted α-helical element comprising residues Leu456 to Trp492. (A) A theoretical 3D model of this helix was built for WT NPR-B (A, left helix) and mutant NPR-B (A, right helix; the deleted residues are marked with C-atoms colored in magenta). The deletion Met482-Leu483 results in a rotational rearrangement of the helix past the deletion site (in panel A, the right panel compares the WT and mutant helix, the rotation is marked). This in silico model suggests that in the mutant NPR-B the residues Glu484 to Trp492 are rotated by 120° clockwise and that the amphipathic structure of the helix is markedly changed. (B) Left panel: 3D model of the helix covering the transmembrane and cytoplasmic submembrane regions is shown for WT and Met482-Leu483del NPR-B (residues Thr451 to Arg495). Color coding was done according to amino acid polarity, with hydrophobic amino acid residues colored in gray, positively charged residues colored in blue, negatively charged residues marked in red, and polar but uncharged amino acids indicated in green. Middle panel: The model is depicted with a semitransparent surface representation showing a continuous hydrophobic patch for Met482-Leu483del past the transmembrane segment. WT NPR-B does not show such a hydrophobic surface patch. Right panel: The model is rotated clockwise by 90° around the y-axis. 3D, 3-dimensional; NPR, natriuretic peptide receptor; WT, wild-type.

preactivated state already in the absence of CNP or a hyperactivated state by stabilizing the CNP-induced active receptor conformation.

Discussion

Loss-of-function sequence variants in NPR-B (encoded by the *NPR2* gene) cause short stature (8-10), whereas gain-of-function variants lead to tall stature (11-13). Here, we describe a mother and 2 daughters with tall stature and macrodactyly of the great toes (epiphyseal chondrodysplasia, Miura type) associated with an in-frame deletion in *NPR2* resulting in the deletion of the amino acids Met482-Leu483 in the intracellular membrane-near region of NPR-B. Assays with cultured native fibroblasts and transfected HEK-293 cells demonstrated that Met482-Leu483del NPR-B responds to CNP with markedly enhanced cGMP production. Also, the ligand-independent (baseline) cGMP-synthesis activity of this mutant receptor is markedly increased. Because the CNP/NPR-B/cGMP signalling pathway is critically involved in bone development by stimulating growth plate chondrocyte differentiation and proliferation (1-3), we conclude that the Met482-Leu483del variant is responsible for the observed skeletal overgrowth of the proband. The current growth of the 2 daughters is not as pronounced compared with the proband. This can be explained by their father's height, which is slightly below average. Because height is a highly polygenic trait, this observation is congruent with the notion that monogenic growth disorders may present with a height within normal ranges.

This report adds to the three earlier reports of gain-of-function NPR-B variants: 2 families with variants in the GCD or submembrane domains exhibited tall stature including macrodactyly of the great toes, scoliosis, coxa valga, and slipped capital femoral epiphysis (11, 12); and 1 man with a variant in the KHD had isolated extreme tall stature (13). Elegant biochemical studies in a heterologous expression system showed that these variants have distinct effects on NPR-B-mediated cGMP production, NPR-B dephosphorylation/desensitization or the allosteric modulation of the GCD by ATP (14, 18). Our comparative studies of the Met482-Leu483del and Arg655Cys NPR-B mutants indicate that the extent of cGMP-overproduction correlates with height (present study and (13)). Ultimately it remains unclear why different activating NPR-B variants are associated with distinct overgrowth phenotypes.

Pronounced macrodactyly of the great toes is a striking feature shared by almost all known gain-of-function NPR-B variants ((11, 12); see Fig. 1 of the present study). In general, 3 cGMP-regulated proteins participate in chondrogenesis and chondrocyte proliferation during long bone growth: cGMP-dependent protein kinases type I and II; and phosphodiesterase (PDE) 3A, a cGMP-inhibited cAMP-hydrolyzing enzyme (1). Notably, during development PDE3A is highly expressed in domains involved in digit formation. PDE3A gain-of-function variants, with increased cAMP-hydrolytic activity, are associated with severe brachydactyly (19). We suggest that augmented CNP/NPR-B/cGMP-dependent inhibition of PDE3A (diminishing cAMP-hydrolytic activity and thereby enhancing chondrocyte cAMP levels) may contribute to macrodactyly in gain-of-function NPR-B variants. However, why overactivation of CNP/NPR-B/cGMP signalling preferentially affects the growth of the big toes is presently unknown.

The proband has a history of delayed puberty, which also occurred in our previous proband (13). This increases final height by allowing for prolonged growth before epiphyseal closure. We assume that in the proband, pubertal delay could have been a result of her low body weight, leading to hypothalamic dysfunction. Another novel clinical feature in this NPR-B gain-of-function phenotype is mesomelia. Until now, this was only reported in loss-of-function NPR-B variants. Unfortunately, segregation analysis of the *NPR2* in-frame deletion with mesomelia or delayed puberty could not be established in other family members. Therefore, it remains unclear if these features are part of the phenotypic spectrum of activating NPR-B variants, and this needs to be explored in future diagnosed families with NPR-B gain-of-function variants.

The presence of pseudo-epiphyses (Fig. 1) has been reported before by Boudin et al. (20), who reviewed X-rays of previously published cases with activating NPR-B variants after they found that biallelic loss-of-function variants in natriuretic peptide receptor-C (NPR-C; also named NPR3) are associated with tall stature, macrodactyly of the great toes, and pseudo-epiphyses (19). NPR-C binds and internalizes all 3 natriuretic peptides (ANP, BNP, CNP) with similar affinities, thereby acting as a "clearance" receptor (1). It was suggested that loss-of-function variants in NPR-C result in reduced clearance of CNP, thereby increasing local CNP levels in the bone and CNP/NPR-B signalling (1, 20).

The reported NPR-B deletion variant Met482-Leu483 as well as the previously reported substitution Ala488Pro (12) affect a topological domain between the transmembrane region and the kinase-homology domain of NPR-B. As shown in Fig. 3, the amino acid sequence of this region is highly conserved in NPR-B across species and among natriuretic peptide receptors.

Notably, both variants resulted in augmented baseline as well as ligand-dependent NPR-B/cGMP activities. Moreover, they were associated with very similar clinical phenotypes, with pronounced macrodactyly of the great toes. Interestingly, a recently published novel NPR-B variant Arg495Cys, affecting the same protein region, was associated with diminished CNP-simulated NPR-B catalytic activity and idiopathic short stature (21). The marked impact of these 3 variants on baseline and CNP-stimulated NPR-B function ((12, 21) and present study) indicates that this submembrane region has a critical role, although the precise function is unknown.

Different NPRs can bind the same ligand (e.g., both NPR-A and NPR-C bind ANP and BNP, both NPR-B and NPR-C bind CNP), indicating that the ECD of all NPRs have similar ligand recognition and activation mechanisms (1). By sedimentation equilibrium analyses, it was found that the crystalized ECD of NPR-A undergoes spontaneous dimerization with a dissociation constant K_d of ~500 nM, suggesting that most NPR-As preexist in the cell's membrane as homodimers (16, 22). Furthermore, crystal structure analyses of the ECDs of NPR-A and NPR-C revealed that a single ANP (in NPR-A) or either ANP or CNP molecule (in NPR-C) binds within the interface of a receptor homodimer and induces a rotation of the ECDs of the 2 dimer subunits with respect to each other (15, 23-25). It is postulated that this movement transduces across the membrane being an allosteric trigger for intracellular signalling by natriuretic peptides (15, 23-25). Such experimental studies have not been performed for NPR-B. However, because of the high amino acid homologies to NPR-A (in the intracellular domains) and NPR-C (in the extracellular domain), it is likely that this allosteric activation mechanism is valid also for NPR-B. To provide a potential molecular explanation for the effect of the described Met482-Leu483 deletion here, we performed in silico modelling of this receptor region. Our 3D model predicted a single uninterrupted α-helical element comprising the transmembrane (Leu456-Phe478) and submembrane regions of NPR-B (until residue Trp492). Because of the architecture of α-helices, the deletion reported here Met482-Leu483 would result in a rotational rearrangement of the helix past the deletion site (clockwise by 120°) and thereby markedly change its amphipathic surface. Based on the results of our functional studies, we assume that this change in amphilicity could stabilize the active conformation of the NPR-B dimer and further facilitate its CNP-induced allosteric activation. This could lead to a hyperactivated state of NPR-B at baseline and upon ligand-binding. However, the exact molecular mechanism is unknown.

Because the probands are heterozygous carriers of the variant, they will possibly express WT/WT (~25%), WT/mut (~50%), and mut/mut (~25%) NPR-B dimers. Our present study and also the previously published studies (11-13) cannot distinguish whether the resulting gain of function of the CNP/NPR-B system is caused by the small population of mut/mut dimers or linked to the prevalent WT/mut dimers.

In summary, with this report of a family with tall stature and macrodactyly of the great toes because of a gain-of-function in-frame deletion within the submembrane region of NPR-B, the genotypical and phenotypical spectrum of NPR-B-related tall stature is expanded. Our observations emphasize the important role of this domain in the regulation of cyclic GMP production and bone growth in response to CNP/NPR-B signaling.

Acknowledgments

The authors are grateful for the participation of the proband and her family.

Financial Support: The studies of CNP/NPR-B signalling by M.K.'s group are funded by the Deutsche Forschungsgemeinschaft (DFG KU 1037/7-1 and DFG KU 1037/8-1) and the Bundesministerium für Forschung und Technik (BMBF 01EO1004). The work of E.B. was supported by grants of the 'Fonds voor Wetenschappelijk Onderzoek Vlaanderen' (12A3814N and 1507317N) and the 'Bijzonder Onderzoeksfonds' (BOF) of the University of Antwerp (BOF KP: 34417).

Author Contributions: P.L., D.v.d.K., M.K., and H.v.D. planned the studies and wrote the manuscript. P.L., A.v.H., and D.v.d.K. gathered clinical data on the proband and her family. Functional assays were performed by E.M.L., E.B., F.W., H.S., and M.K. T.M. performed in silico modellings. All authors critically reviewed manuscript drafts and approved the final manuscripts as submitted.

Additional Information

***Correspondence and Reprint Requests*:** Peter Lauffer, Emma Children's Hospital, Amsterdam University Medical Center, Department of Paediatric Endocrinology, Meibergdreef 9, 1105 AZ Amsterdam, The Netherlands. E-mail: p.lauffer@amsterdamumc.nl.

Disclosure Summary: The authors have no conflicts of interests to state. The authors have no ethical conflicts to disclose. This study was approved by the Medical Ethical Committee of Leiden University Medical Center. The proband and her family agreed to participate and signed informed consent.

Data Availability: The datasets generated during and/or analyzed during the current study are not publicly available but are available from the corresponding author on reasonable request.

References and Notes

1. Kuhn M. Molecular physiology of membrane guanylyl cyclase receptors. *Physiol Rev*. 2016;**96**(2):751-804.
2. Tamura N, Doolittle LK, Hammer RE, Shelton JM, Richardson JA, Garbers DL. Critical roles of the guanylyl cyclase B receptor in endochondral ossification and development of female reproductive organs. *Proc Natl Acad Sci U S A*. 2004;**101**(49):17300-17305.
3. Nakao K, Osawa K, Yasoda A, et al. The Local CNP/GC-B system in growth plate is responsible for physiological endochondral bone growth. *Sci Rep*. 2015;**5**:10554.
4. Schmidt H, Stonkute A, Jüttner R, et al. The receptor guanylyl cyclase Npr2 is essential for sensory axon bifurcation within the spinal cord. *J Cell Biol*. 2007;**179**(2):331-340.
5. Špiranec K, Chen W, Werner F, et al. Endothelial C-type natriuretic peptide acts on pericytes to regulate microcirculatory flow and blood pressure. *Circulation*. 2018;**138**(5):494-508.
6. Potter LR. Guanylyl cyclase structure, function and regulation. *Cell Signal*. 2011;**23**(12):1921-1926.
7. Chusho H, Tamura N, Ogawa Y, et al. Dwarfism and early death in mice lacking C-type natriuretic peptide. *Proc Natl Acad Sci U S A*. 2001;**98**(7):4016-4021.
8. Bartels CF, Bükülmez H, Padayatti P, et al. Mutations in the transmembrane natriuretic peptide receptor NPR-B impair skeletal growth and cause acromesomelic dysplasia, type Maroteaux. *Am J Hum Genet*. 2004;**75**(1):27-34.
9. Vasques GA, Amano N, Docko AJ, et al. Heterozygous mutations in natriuretic peptide receptor-B (NPR2) gene as a cause of short stature in patients initially classified as idiopathic short stature. *J Clin Endocrinol Metab*. 2013;**98**(10):E1636-E1644.
10. Wang SR, Jacobsen CM, Carmichael H, et al. Heterozygous mutations in natriuretic peptide receptor-B (NPR2) gene as a cause of short stature. *Hum Mutat*. 2015;**36**(4):474-481.
11. Miura K, Namba N, Fujiwara M, et al. An overgrowth disorder associated with excessive production of cGMP due to a gain-of-function mutation of the natriuretic peptide receptor 2 gene. *PLoS One*. 2012;**7**(8):e42180.
12. Miura K, Kim OH, Lee HR, et al. Overgrowth syndrome associated with a gain-of-function mutation of the natriuretic peptide receptor 2 (NPR2) gene. *Am J Med Genet A*. 2014;**164A**(1):156-163.
13. Hannema SE, van Duyvenvoorde HA, Premsler T, et al. An activating mutation in the kinase homology domain of the natriuretic peptide receptor-2 causes extremely tall stature without skeletal deformities. *J Clin Endocrinol Metab*. 2013;**98**(12):E1988-E1998.
14. Dickey DM, Otto NM, Potter LR. Skeletal overgrowth-causing mutations mimic an allosterically activated conformation of guanylyl cyclase-B that is inhibited by 2,4,6,-trinitrophenyl ATP. *J Biol Chem*. 2017;**292**(24):10220-10229.
15. Ogawa H, Qiu Y, Ogata CM, Misono KS. Crystal structure of hormone-bound atrial natriuretic peptide receptor extracellular domain: rotation mechanism for transmembrane signal transduction. *J Biol Chem*. 2004;**279**(27):28625-28631.
16. Qiu Y, Ogawa H, Miyagi M, Misono KS. Constitutive activation and uncoupling of the atrial natriuretic peptide receptor by mutations at the dimer interface. Role of the dimer structure in signalling. *J Biol Chem*. 2004;**279**(7):6115-6123.
17. Baeza-Delgado C, Marti-Renom MA, Mingarro I. Structure-based statistical analysis of transmembrane helices. *Eur Biophys J*. 2013;**42**(2–3):199-207.
18. Robinson JW, Dickey DM, Miura K, Michigami T, Ozono K, Potter LR. A human skeletal overgrowth mutation increases maximal velocity and blocks desensitization of guanylyl cyclase-B. *Bone*. 2013;**56**(2):375-382.
19. Maass PG, Aydin A, Luft FC, et al. PDE3A mutations cause autosomal dominant hypertension with brachydactyly. *Nat Genet*. 2015;**47**(6):647-653.
20. Boudin E, de Jong TR, Prickett TCR, et al. Bi-allelic loss-of-function mutations in the npr-c receptor result in enhanced growth and connective tissue abnormalities. *Am J Hum Genet*. 2018;**103**(2):288-295.
21. Hwang IT, Mizuno Y, Amano N, et al. Role of NPR2 mutation in idiopathic short stature: identification of two novel mutations. *Mol Genet Genomic Med*. 2020;**8**(3):e1146.
22. Ogawa H, Qiu Y, Philo JS, Arakawa T, Ogata CM, Misono KS. Reversibly bound chloride in the atrial natriuretic peptide receptor hormone-binding domain: possible allosteric regulation and a conserved structural motif for the chloride-binding site. *Protein Sci*. 2010;**19**(3):544-557.
23. van den Akker F, Zhang X, Miyagi M, Huo X, Misono KS, Yee VC. Structure of the dimerized hormone-binding domain of a guanylyl-cyclase-coupled receptor. *Nature*. 2000;**406**(6791):101-104.
24. He Xl, Chow Dc, Martick MM, Garcia KC. Allosteric activation of a spring-loaded natriuretic peptide receptor dimer by hormone. *Science*. 2001;**293**:1657-1662.
25. Misono KS, Philo JS, Arakawa T, et al. Structure, signaling mechanism and regulation of the natriuretic peptide receptor guanylate cyclase. *Febs J*. 2011;**278**(11):1818-1829.